

## Article

# Antioxidant Quercetin 3-O-Glycosylated Plant Flavonols Contribute to Transthyretin Stabilization

Lidia Ciccone <sup>1,\*</sup> , Nicolò Tonali <sup>2</sup> , Carole Fruchart-Gaillard <sup>3</sup>, Lucia Barlettani <sup>1</sup> , Armando Rossello <sup>1,4</sup>,  
Alessandra Braca <sup>1,5</sup> , Elisabetta Orlandini <sup>4,6</sup> and Susanna Nencetti <sup>1,5</sup> 

<sup>1</sup> Department of Pharmacy, University of Pisa, 56126 Pisa, Italy; l.barlettani@studenti.unipi.it (L.B.); armando.rossello@unipi.it (A.R.); alessandra.braca@unipi.it (A.B.); susanna.nencetti@unipi.it (S.N.)

<sup>2</sup> Centre National de la Recherche Scientifique (CNRS), Biomolécules: Conception, Isolement et Synthèse (BioCIS), Université Paris-Saclay, 92290 Chatenay-Malabry, France; nicolo.tonali@universite-paris-saclay.fr

<sup>3</sup> Département Médicaments et Technologies pour la Santé (DMTS), Service d'Ingénierie Moléculaire pour la Santé (SIMoS), Commissariat à l'Énergie Atomique et aux Énergies Alternatives (CEA), Institut National de Recherche pour l'Agriculture, l'Alimentation et l'Environnement (INRAE), Université Paris Saclay, 91191 Gif-Sur-Yvette, France; carole.fruchart@cea.fr

<sup>4</sup> Research Center "E. Piaggio", Università di Pisa, 56122 Pisa, Italy; elisabetta.orlandini@unipi.it

<sup>5</sup> Interdepartmental Research Centre Nutraceuticals and Food for Health (NUTRAFOOD), University of Pisa, 56126 Pisa, Italy

<sup>6</sup> Department of Earth Sciences, University of Pisa, 56100 Pisa, Italy

\* Correspondence: lidia.ciccone@unipi.it

**Abstract:** Plants are rich in secondary metabolites, which are often useful as a relevant source of nutraceuticals. Quercetin (QUE) is a flavonol aglycone able to bind Transthyretin (TTR), a plasma protein that under pathological conditions can lose its native structure leading to fibrils formation and amyloid diseases onset. Here, the dual nature of five quercetin 3-O-glycosylated flavonol derivatives, isolated from different plant species, such as possible binders of TTR and antioxidants, was investigated. The crystal structure of 3-O-β-D-galactopyranoside in complex with TTR was solved, suggesting that not only quercetin but also its metabolites can contribute to stabilizing the TTR tetramer.

**Keywords:** transthyretin; TTR; quercetin 3-O-glycosylated derivatives; amyloidosis; antioxidant; plant bioactive metabolites; nutraceuticals; phytochemicals



**Citation:** Ciccone, L.; Tonali, N.; Fruchart-Gaillard, C.; Barlettani, L.; Rossello, A.; Braca, A.; Orlandini, E.; Nencetti, S. Antioxidant Quercetin 3-O-Glycosylated Plant Flavonols Contribute to Transthyretin Stabilization. *Crystals* **2022**, *12*, 638. <https://doi.org/10.3390/cryst12050638>

Academic Editors: Ali A. Kermani and Matthew Groves

Received: 4 April 2022

Accepted: 27 April 2022

Published: 29 April 2022

**Publisher's Note:** MDPI stays neutral with regard to jurisdictional claims in published maps and institutional affiliations.



**Copyright:** © 2022 by the authors. Licensee MDPI, Basel, Switzerland. This article is an open access article distributed under the terms and conditions of the Creative Commons Attribution (CC BY) license (<https://creativecommons.org/licenses/by/4.0/>).

## 1. Introduction

Nature is a rich source of bioactive compounds where plant biodiversity contributes to furnishing a large number of nutraceuticals [1]. Quercetin (QUE), related flavonoids and metabolites, are largely studied in vitro and in vivo for their antioxidant, anti-inflammatory, antidiabetic, anticancer and neuroprotective roles [2–6]. Studies report that a diet rich in fruits and vegetables drastically decreases the risk of developing cancer and cardiovascular and degenerative diseases [7–9]. Recently, natural compounds, in particular polyphenols, were investigated for their ability to interact with amyloidogenic proteins contrasting amyloid fibril formation and/or favoring the disaggregation or destabilization of preformed amyloid fibrils [10–14].

Human transthyretin (TTR) is a plasma protein involved in the transport of the thyroid hormone thyroxine (T4) and retinol, through retinol-binding protein, in blood and cerebrospinal fluid (CSF) [15,16]. Moreover, it was reported that TTR can interact with amyloid beta peptides (Aβ), preventing the formation of fibrils aggregates [17–22]. Under the pathological condition, wild-type TTR (wt-TTR) and its variants are involved in amyloid disease onset such as senile systematic amyloidosis (SSA), familial amyloid

polyneuropathy (FAP), familial amyloid cardiomyopathy (FAC) and central nervous system amyloidosis (CNSA).

Deposition of aggregated forms of TTR is responsible of several side effects such as the dysregulation of physiological metals and, consequently, the production of reactive oxygen species (ROS) [23–25]. The relationship between TTR and ROS is not completely understood; however, several studies report that the free thiol of Cys10 is sensitive to oxidation, playing an important role in maintaining the stability of the tetramer [26]. In patients with FAP, the TTR tetramer is characterized by a blend of Cys10-modified species where the ratio between TTR with modified Cys and free Cys is high [27]. This evidence suggests that the destabilization of the TTR structure caused by Cys modification contributes to the abnormal deposition of TTR aggregates [28].

Among several therapeutic strategies against TTR amyloidosis, the stabilization of its tetrameric structure is one of the most studied [29,30]. Currently, two stabilizer drugs, tafamidis meglumine (Vyndaqel<sup>®</sup>) and tafamidis (Vyndimax<sup>TM</sup>), are approved for the treatment of FAC while Diflunisal and AG10 are under clinical studies [31,32].

From a structure point of view, TTR is a 55 kDa homotetrameric protein rich in  $\beta$ -sheets. Each monomer (A, A', B, B') is characterized by four-stranded antiparallel  $\beta$ -sheets and a short  $\alpha$ -helix. Dimer (A-A'/B-B') is formed by two monomers bound together through a hydrogen bond network between the two edge  $\beta$ -strands of each monomer. Two dimers are assembled back to back by hydrophobic contacts to form a central cavity, characterized by two T4 binding pockets that cross the tetramer (Figure 1).

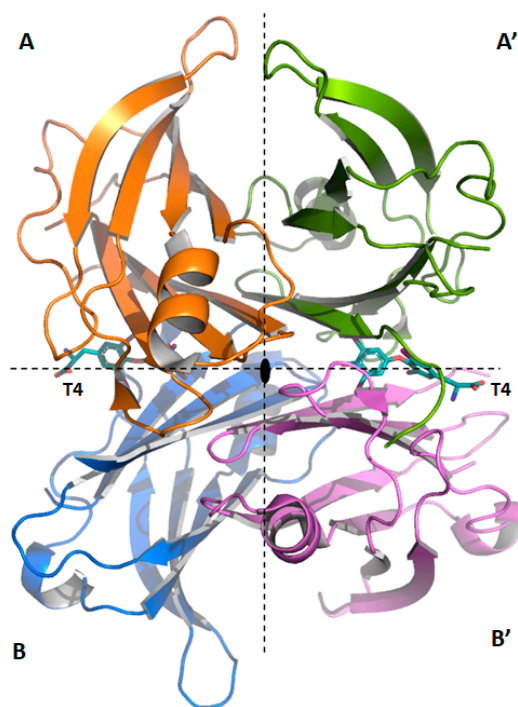


**Figure 1.** Graphic representation of TTR tetramer in complex with T4 (pdb structure 1sn0). The structural figure has been made with PyMol [33] using our in-house script [34].

TTR T4 binding pockets are able to accommodate several classes of natural and synthetic compounds [35,36], stabilizing the tetramer and contrasting the formation of insoluble aggregates. Among the natural flavonoids, it was reported that QUE, a flavonol ubiquitously contained in vegetables and fruits, binds the tetramer ( $IC_{50}$  13.34  $\mu$ M) [37], contrasting the TTR aggregation induced by acid pH. The crystal structure of QUE in complex with wt-TTR confirmed that QUE takes place in one of two T4 binding sites with the dihydroxyphenyl moiety deeply inserted into the pocket and the benzopyran ring pointing towards the outside [38].

It was reported that the ability of glycosylated metabolites to bind TTR tetramer is lower than the aglycone itself [39,40]. QUE also possesses high antioxidant power and is considered a scavenger of free radicals [40,41].

Vegetables and fruits, such as onion, molokheya, broccoli, kale, black tea, orange, blueberry, and apple are rich in QUE and its glycosides derivatives [42]. Therefore, dietary intake includes not only QUE but also its metabolites such as QUE 3-*O*- $\beta$ -D-glucuronopyranoside (1), QUE 3-*O*- $\beta$ -D-galactopyranoside (2), QUE 3-*O*- $\beta$ -D-glucopyranoside (3), QUE 3-*O*- $\alpha$ -L-arabinopyranoside (4) and QUE 3-*O*- $\alpha$ -L-arabinofuranoside (5). In this context, our aim was to investigate if these QUE 3-*O*-glycosydes maintain the ability to bind TTR binding pockets, thus contributing to the tetramer stabilization. Compounds 1–5 were isolated from different plant sources [43–45], and their ability to interact with TTR was evaluated by in vitro assays (turbidimetric assay, ANS competitive binding assay, Thioflavin T fluorescence spectroscopy) and validated by X-ray crystallographic analysis.

As mentioned above, TTR aggregates are related to ROS production, that in turn lead to the destabilization of the tetramer. Thus, starting from the evidence that different studies have reported that QUE 3-*O*- $\beta$ -D-glucuronopyranoside (1), QUE 3-*O*- $\beta$ -D-galactopyranoside (2), QUE 3-*O*- $\beta$ -D-glucopyranoside (3) and QUE 3-*O*- $\alpha$ -L-arabinofuranoside (5) have antioxidant power [46–48], in order to fulfil the QUE 3-*O*-metabolites profile, here the in vitro radical scavenger property of QUE 3-*O*- $\alpha$ -L-arabinopyranoside simultaneously with all isolated glycosylated derivatives, using the DPPH assay, was evaluated.

## 2. Materials and Methods

### 2.1. In Vitro Studies

#### 2.1.1. Turbidimetric Assay

The turbidimetric assay was carried out following the protocol previously described [49]. Lyophilized Prealbumin, Human Plasma (wt-TTR) was purchased from Merck Millipore (Molsheim, France). 3-*O*-glycosylated derivatives, isolated from *Cornus mas*, *Cornus sanguinea*, and *Ruprechtia polystacya* [43,45], were dissolved in DMSO (7.2 mM), and the stock solution was diluted to reach a final concentration of 1.44 mM. A stock solution of TTR at 7.2  $\mu$ M was made using 10 mM phosphate buffer pH 7.6 (100 mM KCl, 1.7 mM EDTA). The TTR solution was dispensed into wells of 96-well microplate, and the stock stabilizer solution, or DMSO for the negative control, was added. The plate was incubated for 30 min at r.t. After the incubation, acetate buffer (200 mM acetate at pH 4.4, 100 mM KCl, 1.7 mM EDTA) was aliquoted in each well. The microplate was incubated at 37 °C for 72 h without stirring, then the plate was vortexed, and the optical density was measured at 450 nm using a SPECTROstarNano (200–1000 nm) UV/Vis spectrophotometer. All compounds were tested in triplicate and the percentage of fibril formation was calculated as previously described [50].

#### 2.1.2. Thioflavin T Fluorescence Assay (ThT)

An in vitro ThT fluorescence assay was performed in accordance with the protocol already described [51]. In brief, wt-TTR (7.2  $\mu$ M), purchased from Calbiochem (EDM Millipore, cat.529577 lot: 2896620), was incubated overnight at 37 °C in 10 mM phosphate buffer (pH 7.0) in the presence or in the absence of 10  $\mu$ M 3-*O*-glycosylated derivatives (1–5). 200 mM acetate buffer (pH 4.4) containing 1 mM EDTA and 100 mM KCl were mixed and incubated at 37 °C for 96 h (final concentration of TTR 3.6  $\mu$ M). After incubation, amyloid fibril formation was assessed by a ThT binding assay (10  $\mu$ M ThT in 50 mM glycine buffer pH 9; TTR concentration at 0.045  $\mu$ M) after incubation at 37 °C for 30 min. Bars are representative of the 9 dilution measurements from the same incubation vial. Values represent the mean  $\pm$  the standard error.

### 2.1.3. ANS Competitive Binding Assay

#### Recombinant Expression of TTR in *E. coli*

TTR protein production was conducted using an *Escherichia coli* expression system previously described [51]. The purification of TTR on Size-exclusion chromatography (SEC) Sephacryl<sup>®</sup> S-100 HR GE Healthcare in buffer 100 mM Tris HCl pH 8, 150 mM NaCl. TTR was concentrated at 3.69 mg/mL.

#### ANS Competitive Binding Assay

The binding of ANS (8-anilino-1-naphthalenesulfonic acid, SigmaAldrich (St. Louis, MO, USA) and its displacement by the five 3-*O*-glycosylated derivatives (1–5) were studied using recombinant wt-TTR protein. TTR (2  $\mu$ M, phosphate buffer (PB) 100 mM, pH 7.5) was incubated with ANS (4  $\mu$ M, PB, 100 mM, pH 7.5) at r.t. for 15 min in 96-well plates. Then, compounds 1–5 at different concentrations (100  $\mu$ M to 50  $\mu$ M) were added. After 10 min, the plate was stirred, and the fluorescent emission spectra (400–540 nm) were recorded by exciting at 280 nm [52] using Molecular Devices SpectraMax Gemini XPS plate reader. In all experiments, the fluorescence increases of ANS bound to TTR solution compared to its control without TTR, and TTR alone, in PB buffer, were used as a control.

### 2.2. Crystallogenes and Structure Resolution

Crystallization experiments were carried out with Lyophilized Prealbumin Merck Millipore (Molsheim, France). The co-crystallization trials were performed by sitting drop vapor diffusion using Cryst Chem<sup>TM</sup> plates: 1  $\mu$ L drop of protein mixed with derivatives (1–5) and 1  $\mu$ L drop of precipitant, stored in a constant temperature incubator at 20 °C. The TTR–3-*O*- $\beta$ -D-galactopyranoside (2) crystal complex was prepared from TTR at 5.02 mg/mL and 10 mM of ligands dissolved in DMSO, in a volumetric ratio of 6:1, according to the previously reported strategy [53]. All crystals were obtained mixing 80% of commercial solution #2\_4.D (30% PEG 4000, 0.2 M Imidazole Malate pH 6.0) with 15% of solution #2\_5.A (12% MPEG 5000, 0.1 Sodium Acetate pH 5.5) of Stura Footprint Screen (Molecular Dimensions Ltd., Cambridge, UK). For X-ray data collection, the crystals were cryoprotected by soaking cryoprotectant solution composed of 40% of CM16 according to the protocol previously described [54]. In order to avoid the leakage of the ligand during the flash cool in liquid nitrogen, the stabilizers were added to the cryoprotectant solution and soaked for 30 min at room temperature [55]. The data sets for the TTR–ligands crystal complexes were collected on the beamline PROXIMA 2A at Synchrotron SOLEIL storage ring in St. Aubin, France [56]. The MX data collections were carried out using microfocused X-rays (FWHM 10  $\mu$ m  $\times$  5  $\mu$ m) using both helical scan and standard rotation methods [56,57]. Data processing was carried out using XDS with the “xdsme” script (<https://github.com/legrandp/xdsme> (accessed on 2 February 2022)) to optimize data quality. Molecular replacement was carried out using MolRep [58]. The ligand restraint file was built using the smiles code in phenix.elbow [59] or with the monomer library sketcher from the CCP4 package [58]. The electron density maps were viewed and fitted in COOT [60]. The structures were subjected to various cycles of rebuilding and refinement with RefMac and PHENIX [58,59]. The figures were made with PyMOL [33].

### 2.3. 2,2-Diphenyl-1-Picrylhydrazyl (DPPH) Radical Scavenging

The DPPH assay was carried out in a 96-microwell plate (200  $\mu$ L), following a previously described protocol [61,62]. In total, 195  $\mu$ L of freshly prepared DPPH solution (60  $\mu$ M in MeOH) was added with 5  $\mu$ L of compounds 1–5 or MeOH as the control. The plate was incubated in the dark for 1 h at r.t. The absorbance was measured at 517 nm using a SPECTROstarNano (200–1000 nm) UV/Vis spectrophotometer.

Glycosylated derivatives 1–5 were tested in triplicate. Serial solutions were carried out with the stock solution (10 mM in MeOH) from 50  $\mu$ M and 1  $\mu$ M. The percentage of the

antioxidant activity (AA) of the compounds was determined according to the following Equation (1):

$$\%AA = ((Abs_{DPPH} - Abs_{sample}) / Abs_{DPPH}) \times 100 \quad (1)$$

$Abs_{DPPH}$  is the absorbance of DPPH solution, and  $Abs_{sample}$  is the absorbance of DPPH solution containing the test compound.

The concentration of tested compounds that decreased 50% of free radical concentration ( $RC_{50}$ ) was calculated for compounds 1–5.

### 3. Results and Discussion

Glycosylated derivatives 1–5 (Figure 2) were screened as potential stabilizers of wt-TTR amyloidogenesis using a turbidity assay [49].

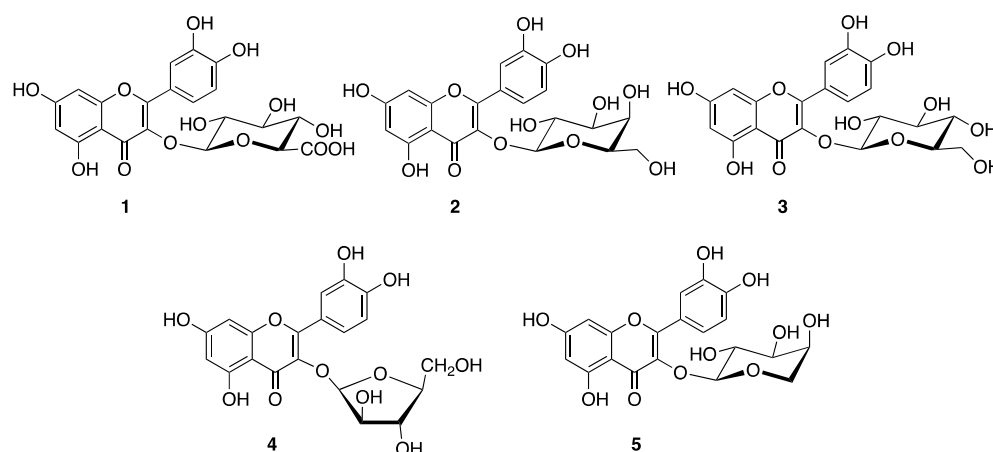


**Figure 2.** Chemical structures of flavonol quercetin derivatives 1–5.

Fibril formation is reported relative to wt-TTR homotetramer, where the amount of aggregation in the absence of a stabilizer is assigned to be 100%. Therefore, 5% fibril formation (FF) in the presence of the reference drug diflunisal corresponds to 95% inhibition, Figure 3. QUE glycoside derivatives showed moderate activity as a stabilizer of FF. The percentage of fibril formation (%FF) of wt-TTR in the presence of QUE 3-O- $\alpha$ -L-arabinofuranoside (5) is 57%, suggesting that derivative (5) has poor interaction with TTR binding sites. However, the %FF decreases from 45%, for QUE 3-O- $\beta$ -D-glucuronopyranoside (1) and QUE 3-O- $\beta$ -D-glucopyranoside (3), to 40% for QUE 3-O- $\beta$ -D-galactopyranoside (2) and QUE 3-O- $\alpha$ -L-arabinopyranoside (4) (Figure 2).

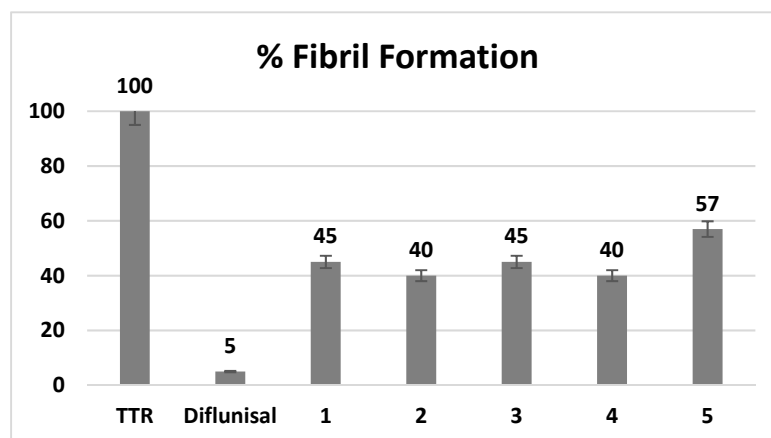


**Figure 3.** In vitro acid turbidimetric assay of wt-TTR. Histogram shows the percentages of aggregate formation related to glycoside derivatives 1–5. The fibril formation in the absence of a stabilizer was assigned to be 100%. The error in the fibril formation assay is  $\pm 5\%$ .

The turbidimetric investigation highlighted that the glycosylated derivatives 1–5 showed a weak ability to inhibit the TTR FF process, thus suggesting a weak interaction with T4 binding sites. An average of around 50% of fibril formation was observed for all the compounds, with the glycosylated derivative 5 as the less effective.

The inhibition activity against the TTR aggregation of derivatives 1–5 was also investigated by a Thioflavin T (ThT) binding assay. As shown in Figure 4, the ThT test, which is more precise in detecting the formation of  $\beta$ -sheet rich aggregate structures, confirmed the inhibitory activity of derivatives 1–3 with a reduction of the fibril formation between 23% and 38%, compared to TTR. However, in the presence of derivatives 4 and 5, containing an arabinopyranoside or arabinofuranoside, TTR seems to be more aggregative and increases the fibril formation. This last result seems in contradiction with the previous turbidity assay. The discrepancy of the data might be related to the fact that the ThT test is able to detect even small, still soluble protofibrils, so very well structured in a  $\beta$ -sheet manner that the rotation around the  $\sigma$  bond of the dye is blocked, with the enhancement of the fluorescence emission as a consequence. These small soluble protofibrils, however, are not so big to increase the turbidity of the solution.

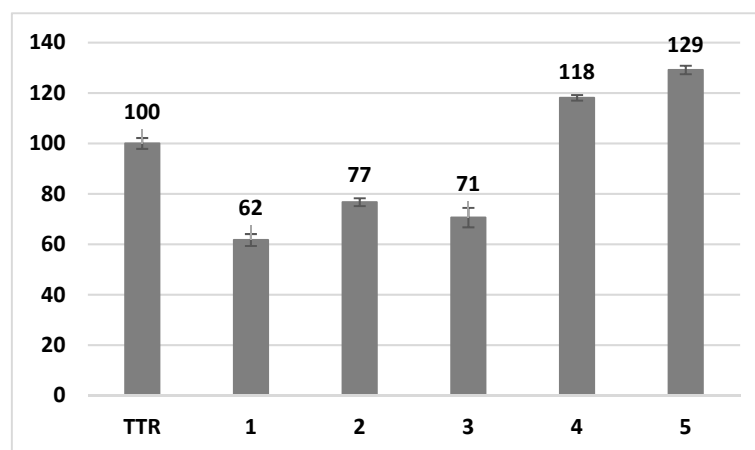


**Figure 4.** In vitro ThT fluorescence assay of wt-TTR in the absence or in the presence of derivatives 1–5. Histogram shows the percentages of aggregate formation. The fibril formation in the absence of a stabilizer was assigned to be 100%. Values represent the mean  $\pm$  the standard error.

To evaluate if glycosylated QUE derivatives 1–5 were able to interact with the TTR binding sites, the ANS displacement binding assay was performed. ANS is one of the most known fluorophores capable of binding simultaneously both TTR binding sites [63]; thus, when a tested compound provokes the quenching of the TTR-ANS fluorescence complex, it means that the molecules studied displaces ANS out of TTR binding sites. In agreement with the other results, the addition of compounds 1–5 slightly decreases the TTR-ANS fluorescence at a concentration of 100  $\mu$ M (Figure 5). The high concentration needed for the ANS displacement is due to the poor affinity of the glycosylated derivatives for the binding sites.

In order to verify the ability of compounds 1–5 to interact with TTR tetramer, a co-crystallogenesis screening of all glycosylated derivatives with wt-TTR was performed. A good ligand density was only obtained for QUE 3-O- $\beta$ -D-galactopyranoside (2) (Figure S1). The TTR-QUE 3-O- $\beta$ -D-galactopyranoside crystal complex belongs to the orthorhombic space group  $P2_12_12$  with cell parameters  $a = 43.230$ ,  $b = 85.600$ ,  $c = 64.430$ ;  $\alpha = \beta = \gamma = 90^\circ$ , Table 1.

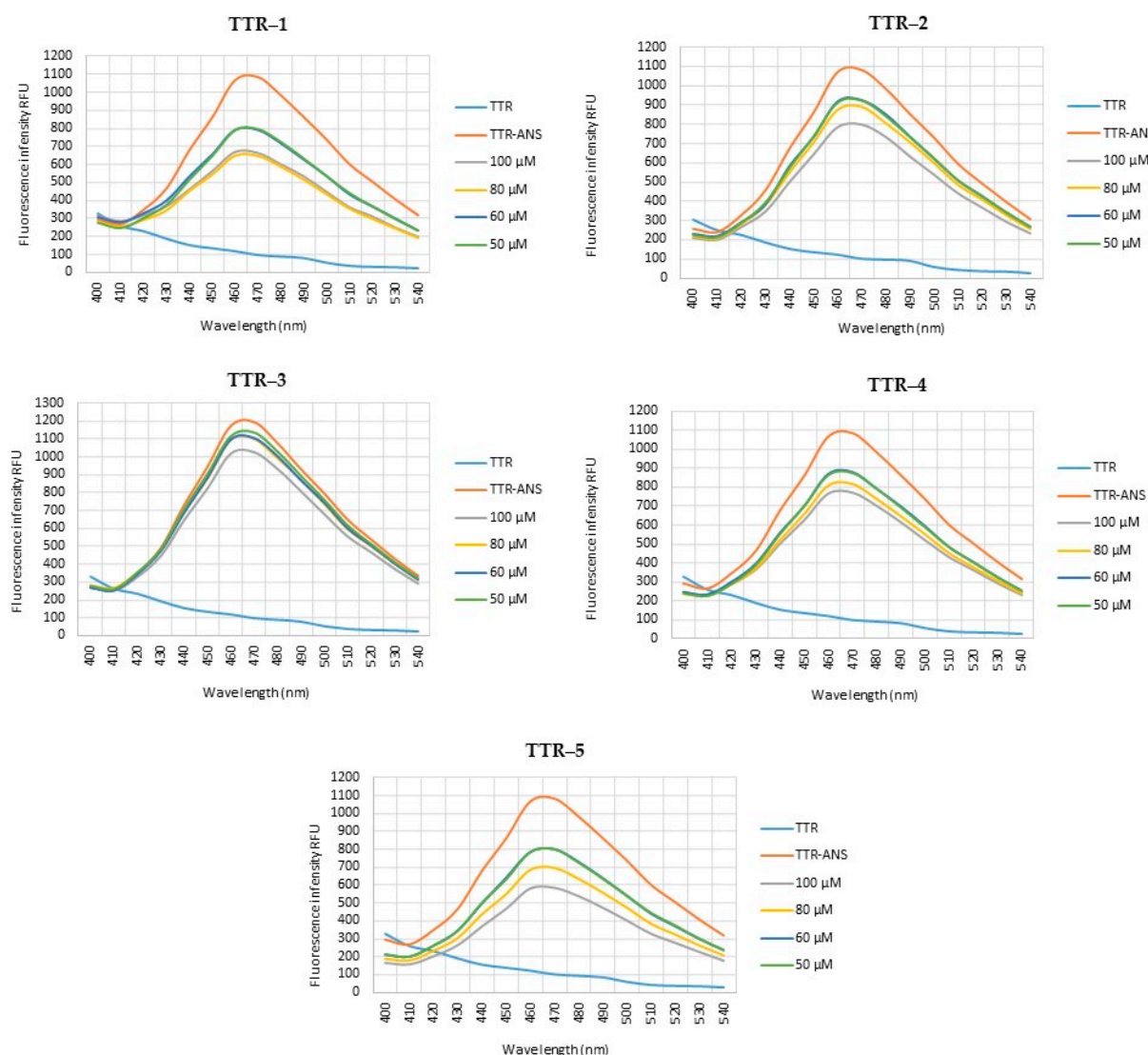


**Figure 5.** Displacement of ANS by glycosylated derivatives 1–5. TTR was incubated in the absence or presence of ANS (ratio 1:2) for 15 min. TTR-ANS complex was added after different concentrations (100  $\mu\text{M}$ , 80  $\mu\text{M}$ , 60  $\mu\text{M}$  and 50  $\mu\text{M}$ ) of compounds 1–5. The fluorescence emission spectra (400–540 nm) were recorded by exciting at 280 nm.

The binding of the ligand to the protein was immediately detected by the yellow color on the crystal obtained (Figure 6A). In the X-ray TTR–QUE 3-*O*- $\beta$ -D-galactopyranoside crystal structure, the additional electro density related to the binding of the ligand (2) was detectable only in pocket B/B' (Figure 6A,B). Since QUE 3-*O*- $\beta$ -D-galactopyranoside binds along the two-fold axis of the tetramer, the ligand occupancy was fixed at 0.5. The two TTR monomers A and B, in the asymmetric unit, have only minor differences.

The weak binding affinity of QUE 3-*O*- $\beta$ -D-galactopyranoside 2 with the TTR pocket could be explained by comparing its binding mode (crystal structure code 7Z60) with that of quercetin (pdb code 4WNJ) [38] (Figure 6C–E). In both structures, ligands are bound only in the binding pocket located at the interface of monomer B/B'. This evidence is in accordance with the data obtained by the ANS displacement binding assay, where compound 2 and its analogues probably replace only one of the two molecules of ANS bound to T4-binding sites. In the TTR-quercetin crystal complex, the benzopyran ring of quercetin is located in the outer binding pocket pointing Lys15 (Figure 6C–E), while the OH- groups of the dihydroxyphenyl ring are oriented towards the inner binding pocket Ser117 and Thr119 (Figure 6D). Compound 2 showed an opposite orientation in the TTR binding pocket. The

benzopyran ring points toward the inner binding pocket while the dihydroxyphenyl ring is situated in the outer binding pocket orienting the galactopyranoside moiety towards the exit of the channel (Figure 6D,E). The ligands superposition clearly shows that QUE 3-O- $\beta$ -D-galactopyranoside **2** is slightly more out of the pocket with respect to quercetin, and this is probably due to the steric hindrance of the galactopyranoside group.

**Table 1.** TTR-2 crystal complex: crystallization, data collection, processing and refinement.

Structure	TTR–QUE 3-O- $\beta$ -D-Galactopyranoside Crystal Complex
PDB code	7Z60
Crystallization	80% (30% PEG 4000, 0.2 M Imidazole Malate pH 6.0) and 15% (12% MPEG 5000, 0.1 Sodium Acetate pH 5.5)
<b>Data Collection</b>	
Source	SOLEIL PROXIMA2A
Wavelength (Å°)	0.980
Space group	$P2_12_12$
Unit-cell (Å°)	$a = 43.230, b = 85.600, c = 64.430; \alpha = \beta = \gamma = 90^\circ$
Molec./asym.	2
Resolution (Å°)	42.80–1.40/1.43–1.40
CC1/2 (%)	99.9/39.6
$\langle I/\sigma(I) \rangle$	18.10/0.93
No. of reflections	569968
No. of unique reflections	45603
Completeness (%)	99.7/93.0
Multiplicity	13.3/13.3
Refinement	Refmac
Resolution (Å°)	42.80–1.40/1.43–1.40
No. of reflections	45603
R-work	18.23
R-free	21.9
RMSD Bond lengths (Å°)	0.01
RMSD Bond angles (°)	1.75
Ramachandran favored	96.60%
Ramachandran outliers	0

Structural analysis is in accordance with all previous results supporting the evidence that QUE 3-O- $\beta$ -D-galactopyranoside is able to bind into the TTR pocket, but the presence of the galactopyranoside in position 3 forces the orientation of the ligand slightly out of the binding site.

The antioxidant activity of each compound is expressed as  $RC_{50}$  (the concentration of tested compounds that decreased 50% of free radical concentration) and is related to its interaction with the free stable radical 2,2-diphenyl-1-picrylhydrazyl (DPPH•). All derivatives possess a good profile as radical scavengers (Table 2), and the data related to compounds **1–3** and **5** are in agreement with those reported in the literature [46–48].

**Table 2.** Antioxidant activity based on DPPH radical scavenging method.

Compounds	Radical Scavenging Activity <sup>a</sup> $RC_{50}$ ( $\mu$ M)	R <sup>2</sup>
Quercetin	$5.4 \pm 1.0$ [66]	0.989
<b>1</b>	$4.78 \pm 1.07$	0.997
<b>2</b>	$24.96 \pm 1.09$	0.988
<b>3</b>	$4.47 \pm 1.09$	0.978
<b>4</b>	$29.40 \pm 1.08$	0.987
<b>5</b>	$5.62 \pm 1.08$	0.995

<sup>a</sup> Mean  $\pm$  SD of three independent experiment for 50% antioxidant activity.

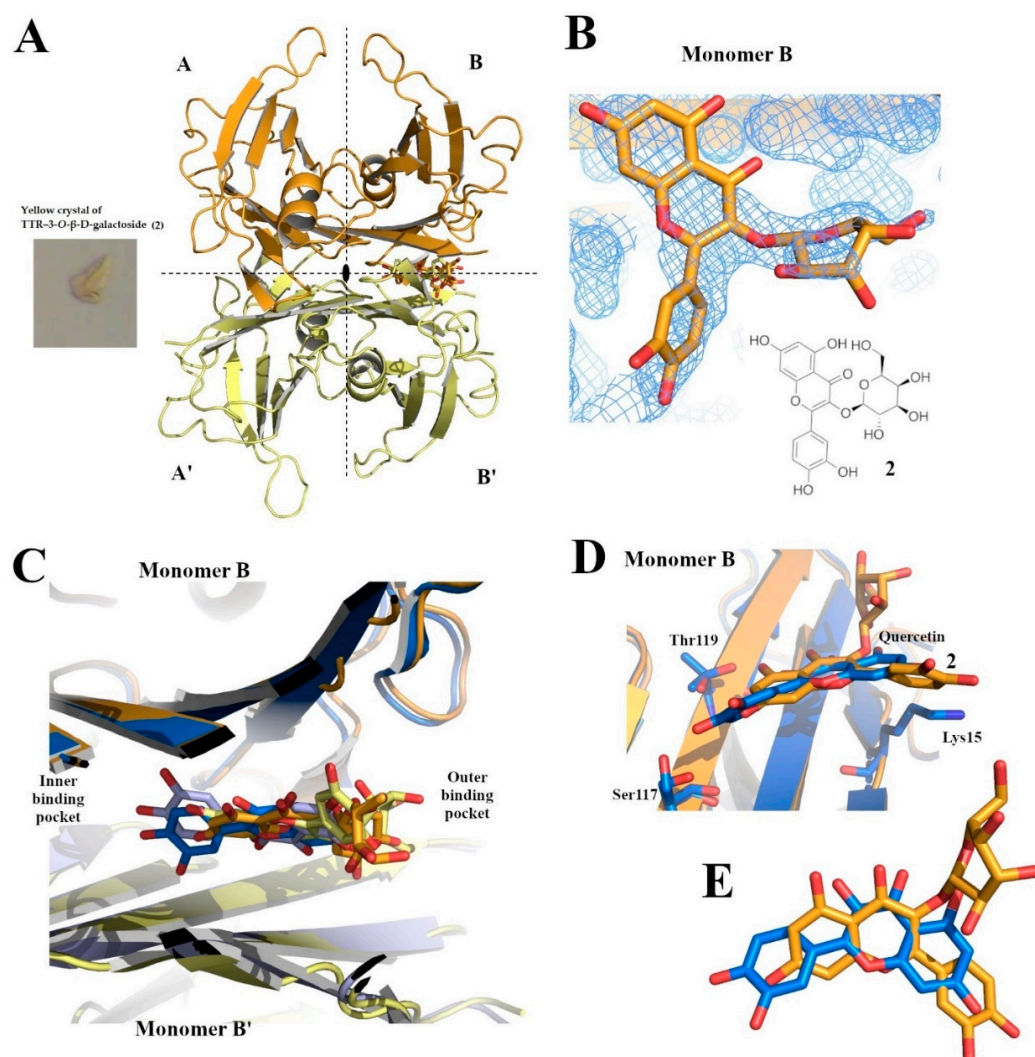


**Figure 6.** Graphic representation of QUE 3-O-β-D-galactopyranoside in complex with wt-TTR. (A) QUE 3-O-β-D-galactopyranoside bound to TTR tetramer binding site B/B'. (B) Zoom of ligand contoured by its electron density (weighted 2Fo-Fc, contoured at 1.0  $\sigma$ ). Chemical structure of compound 2. (C) Superposition between the crystal structure of quercetin complexed with wt-TTR (pdb code 4WNJ) colored in marine and light blue (symmetric) and TTR-QUE 3-O-β-D-galactopyranoside complex (bright orange and pale yellow symmetric). (D) Comparison between the two ligands in T4-TTR binding site (QUE colored marine and QUE 3-O-β-D-galactopyranoside in bright orange). (E) Zoom of ligands superposition (QUE colored marine and QUE 3-O-β-D-galactopyranoside in bright orange). Structural figures have been made with PyMol [33], modifying the scripts previously used [64], and the images were assembled using GNU Image Manipulation Program (GIMP) [65].

It is interesting to underline that, even if derivatives 1–5 do not show a relevant ability to bind T4 binding sites, they possess high antioxidant power that could contribute to contrast the oxidation of Cys10, favoring the maintenance of the TTR tetrameric structure.

#### 4. Conclusions

Natural compounds are a huge source of bioactive and nutraceutical products with benefits against amyloid diseases [14,67,68]. Moreover, it is well known that a diet rich in fruits and vegetables reduces the incidence of degenerative disease onset and progression.

In this context, starting from the evidence that QUE is a flavonol aglycone able to bind and stabilize TTR tetramer, the aim of this work was to study whether not only QUE but also its natural 3-O-glycosylated metabolites 1–5, largely present in plants as secondary

metabolites, were able to interact with TTR. It is known that QUE and its derivatives possess high antioxidant power; thus, they can potentially contribute to reducing oxidative stress related to TTR aggregates, contrasting the oxidation of Cys10 involved in maintaining tetramer stability.

The data reported here suggest that QUE 3-O-glycosylated derivatives 1–5 interact with T4 binding pockets. The in vitro turbidimetric, ThT and ANS fluorescence binding assays show that the five QUE glycosylated derivatives are able to interact with the TTR tetramer slightly, contributing to the tetramer stabilization. Analyzing the crystal complex of compound 2 in complex with TTR, it is reasonable to think that this is probably due to the glycosidic group in position three that impedes a good allocation of the natural flavonol 2 into the binding sites. The QUE 3-O-glycosylated plant flavonols can strengthen the beneficial effects that QUE has on TTR stabilization, both binding into the T4 binding site and contrasting the oxidative stress, characteristic of TTR aggregates, which leads to tetramer misfolding.

**Supplementary Materials:** The following supporting information can be downloaded at: <https://www.mdpi.com/article/10.3390/cryst12050638/s1>, Figure S1: OMIT map of QUE 3-O- $\beta$ -D-galactopyranoside.

**Author Contributions:** Conceptualization, S.N., L.C. and E.O.; methodology, A.R., A.B. and N.T.; software, L.C. and L.B.; resources C.F.-G. and A.B.; writing—original draft preparation, L.C.; writing—review and editing, N.T., S.N., E.O., A.B. and A.R. All authors have read and agreed to the published version of the manuscript.

**Funding:** This research was funded by the Italian Ministero dell’Istruzione, dell’Università e della Ricerca (PRIN 2017SNRXH3).

**Data Availability Statement:** Not applicable.

**Acknowledgments:** The authors acknowledge the team of PROXIMA2A beamline, Synchrotron SOLEIL, France, for their support during data collection.

**Conflicts of Interest:** The authors declare no conflict of interest.

## References

1. Souyoul, S.A.; Saussy, K.P.; Lupo, M.P. Nutraceuticals: A Review. *Dermatol. Ther.* **2018**, *8*, 5–16. [[CrossRef](#)]
2. Lu, J.; Wang, Z.; Li, S.; Xin, Q.; Yuan, M.; Li, H.; Song, X.; Gao, H.; Pervaiz, N.; Sun, X.; et al. Quercetin Inhibits the Migration and Invasion of HCCLM3 Cells by Suppressing the Expression of P-Akt1, Matrix Metalloproteinase (MMP) MMP-2, and MMP-9. *Med. Sci. Monit.* **2018**, *24*, 2583–2589. [[CrossRef](#)]
3. Kawabata, K.; Mukai, R.; Ishisaka, A. Quercetin and Related Polyphenols: New Insights and Implications for Their Bioactivity and Bioavailability. *Food Funct.* **2015**, *6*, 1399–1417. [[CrossRef](#)]
4. Salehi, B.; Machin, L.; Monzote, L.; Sharifi-Rad, J.; Ezzat, S.M.; Salem, M.A.; Merghany, R.M.; El Mahdy, N.M.; Kılıç, C.S.; Sytar, O.; et al. Therapeutic Potential of Quercetin: New Insights and Perspectives for Human Health. *ACS Omega* **2020**, *5*, 11849–11872. [[CrossRef](#)]
5. Ciccone, L.; Vandooren, J.; Nencetti, S.; Orlandini, E. Natural Marine and Terrestrial Compounds as Modulators of Matrix Metalloproteinases-2 (MMP-2) and MMP-9 in Alzheimer’s Disease. *Pharmaceuticals* **2021**, *14*, 86. [[CrossRef](#)]
6. Alizadeh, S.R.; Ebrahimzadeh, M.A. O-Glycoside Quercetin Derivatives: Biological Activities, Mechanisms of Action, and Structure–Activity Relationship for Drug Design, a Review. *Phytother. Res.* **2022**, *36*, 778–807. [[CrossRef](#)]
7. Wang, D.D.; Li, Y.; Bhupathiraju, S.N.; Rosner, B.A.; Sun, Q.; Giovannucci, E.L.; Rimm, E.B.; Manson, J.E.; Willett, W.C.; Stampfer, M.J.; et al. Fruit and Vegetable Intake and Mortality. *Circulation* **2021**, *143*, 1642–1654. [[CrossRef](#)]
8. van der Merwe, M. Gut Microbiome Changes Induced by a Diet Rich in Fruits and Vegetables. *Int. J. Food Sci. Nutr.* **2021**, *72*, 665–669. [[CrossRef](#)]
9. López-González, L.; Becerra-Tomás, N.; Babio, N.; Martínez-González, M.Á.; Díaz-López, A.; Corella, D.; Goday, A.; Romaguera, D.; Vioque, J.; Alonso-Gómez, Á.M.; et al. Variety in Fruits and Vegetables, Diet Quality and Lifestyle in an Older Adult Mediterranean Population. *Clin. Nutr.* **2021**, *40*, 1510–1518. [[CrossRef](#)]
10. Bieschke, J. Natural Compounds May Open New Routes to Treatment of Amyloid Diseases. *Neurotherapeutics* **2013**, *10*, 429–439. [[CrossRef](#)]
11. Ferreira, N.; Saraiva, M.J.; Almeida, M.R. Natural Polyphenols Inhibit Different Steps of the Process of Transthyretin (TTR) Amyloid Fibril Formation. *FEBS Lett.* **2011**, *585*, 2424–2430. [[CrossRef](#)]

12. Ortore, G.; Orlandini, E.; Braca, A.; Ciccone, L.; Rossello, A.; Martinelli, A.; Nencetti, S. Targeting Different Transthyretin Binding Sites with Unusual Natural Compounds. *ChemMedChem* **2016**, *11*, 1865–1874. [[CrossRef](#)]
13. Pagano, K.; Tomaselli, S.; Molinari, H.; Ragona, L. Natural Compounds as Inhibitors of A $\beta$  Peptide Aggregation: Chemical Requirements and Molecular Mechanisms. *Front. Neurosci.* **2020**, *14*, 1384. [[CrossRef](#)]
14. Ahmad, S.S.; Younis, K.; Philippe, J.; Aschner, M.; Khan, H. Strategic Approaches to Target the Enzymes using Natural Compounds for the Management of Alzheimer’s Disease: A Review. Available online: <https://www.ingentaconnect.com/content/ben/cnsnddt/pre-prints/content-34382514> (accessed on 15 March 2022).
15. Buxbaum, J.N.; Reixach, N. Transthyretin: The Servant of Many Masters. *Cell. Mol. Life Sci.* **2009**, *66*, 3095–3101. [[CrossRef](#)]
16. Liz, M.A.; Mar, F.M.; Franquinho, F.; Sousa, M.M. Aboard Transthyretin: From Transport to Cleavage. *IUBMB Life* **2010**, *62*, 429–435. [[CrossRef](#)]
17. Vieira, M.; Saraiva, M.J. Transthyretin: A Multifaceted Protein. *BioMolecular Concepts* **2014**, *5*, 45–54. [[CrossRef](#)]
18. Garai, K.; Posey, A.E.; Li, X.; Buxbaum, J.N.; Pappu, R.V. Inhibition of Amyloid Beta Fibril Formation by Monomeric Human Transthyretin. *Protein Sci.* **2018**, *27*, 1252–1261. [[CrossRef](#)]
19. Ciccone, L.; Fruchart-Gaillard, C.; Mourier, G.; Savko, M.; Nencetti, S.; Orlandini, E.; Servent, D.; Stura, E.A.; Shepard, W. Copper Mediated Amyloid- $\beta$  Binding to Transthyretin. *Sci. Rep.* **2018**, *8*, 13744. [[CrossRef](#)]
20. Ciccone, L.; Shi, C.; di Lorenzo, D.; Van Baelen, A.-C.; Tonali, N. The Positive Side of the Alzheimer’s Disease Amyloid Cross-Interactions: The Case of the A $\beta$  1–42 Peptide with Tau, TTR, CysC, and ApoA1. *Molecules* **2020**, *25*, 2439. [[CrossRef](#)]
21. Ashrafian, H.; Zadeh, E.H.; Khan, R.H. Review on Alzheimer’s Disease: Inhibition of Amyloid Beta and Tau Tangle Formation. *Int. J. Biol. Macromol.* **2021**, *167*, 382–394. [[CrossRef](#)]
22. Alemi, M.; Gaiteiro, C.; Ribeiro, C.A.; Santos, L.M.; Gomes, J.R.; Oliveira, S.M.; Couraud, P.-O.; Weksler, B.; Romero, I.; Saraiva, M.J.; et al. Transthyretin Participates in Beta-Amyloid Transport from the Brain to the Liver- Involvement of the Low-Density Lipoprotein Receptor-Related Protein 1? *Sci. Rep.* **2016**, *6*, 20164. [[CrossRef](#)]
23. Fong, V.H.; Vieira, A. Cytotoxic Effects of Transthyretin Aggregates in an Epidermoid Cell Line. *PAT* **2017**, *84*, 218–222. [[CrossRef](#)]
24. Teixeira, P.F.; Cerca, F.; Santos, S.D.; Saraiva, M.J. Endoplasmic Reticulum Stress Associated with Extracellular Aggregates: Evidence from Transthyretin Deposition in Familial Amyloid Polyneuropathy. *J. Biol. Chem.* **2006**, *281*, 21998–22003. [[CrossRef](#)]
25. Wieczorek, E.; Ozyhar, A. Transthyretin: From Structural Stability to Osteoarticular and Cardiovascular Diseases. *Cells* **2021**, *10*, 1768. [[CrossRef](#)]
26. Pereira, C.D.; Minamino, N.; Takao, T. Free Thiol of Transthyretin in Human Plasma Most Accessible to Modification/Oxidation. *Anal. Chem.* **2015**, *87*, 10785–10791. [[CrossRef](#)]
27. Hanyu, N.; Shimizu, T.; Yamauchi, K.; Okumura, N.; Hidaka, H. Characterization of Cysteine and Homocysteine Bound to Human Serum Transthyretin. *Clin. Chim. Acta* **2009**, *403*, 70–75. [[CrossRef](#)]
28. Sharma, M.; Khan, S.; Rahman, S.; Singh, L.R. The Extracellular Protein, Transthyretin Is an Oxidative Stress Biomarker. *Front. Physiol.* **2019**, *10*, 5. [[CrossRef](#)]
29. Obici, L.; Mussinelli, R. Current and Emerging Therapies for Hereditary Transthyretin Amyloidosis: Strides Towards a Brighter Future. *Neurotherapeutics* **2021**, *18*, 2286–2302. [[CrossRef](#)]
30. Park, G.Y.; Jamerlan, A.; Shim, K.H.; An, S.S.A. Diagnostic and Treatment Approaches Involving Transthyretin in Amyloidogenic Diseases. *Int. J. Mol. Sci.* **2019**, *20*, 2982. [[CrossRef](#)]
31. Elliott, P.; Drachman, B.M.; Gottlieb, S.S.; Hoffman, J.E.; Hummel, S.L.; Lenihan, D.J.; Ebede, B.; Gundapaneni, B.; Li, B.; Sultan, M.B.; et al. Long-Term Survival With Tafamidis in Patients With Transthyretin Amyloid Cardiomyopathy. *Circ. Heart Fail.* **2022**, *15*, e008193. [[CrossRef](#)]
32. Nelson, L.T.; Paxman, R.J.; Xu, J.; Webb, B.; Powers, E.T.; Kelly, J.W. Blinded Potency Comparison of Transthyretin Kinetic Stabilisers by Subunit Exchange in Human Plasma. *Amyloid* **2021**, *28*, 24–29. [[CrossRef](#)]
33. Lill, M.A.; Danielson, M.L. Computer-Aided Drug Design Platform Using PyMOL. *J. Comput. Aided Mol. Des.* **2011**, *25*, 13–19. [[CrossRef](#)]
34. Ciccone, L.; Tonali, N.; Nencetti, S.; Orlandini, E. Natural Compounds as Inhibitors of Transthyretin Amyloidosis and Neuroprotective Agents: Analysis of Structural Data for Future Drug Design. *J. Enzym. Inhib. Med. Chem.* **2020**, *35*, 1145–1162. [[CrossRef](#)]
35. Guo, X.; Liu, Z.; Zheng, Y.; Li, Y.; Li, L.; Liu, H.; Chen, Z.; Wu, L. Review on the Structures and Activities of Transthyretin Amyloidogenesis Inhibitors. *DDDT* **2020**, *14*, 1057–1081. [[CrossRef](#)]
36. Trivella, D.B.B.; dos Reis, C.V.; Lima, L.M.T.R.; Foguel, D.; Polikarpov, I. Flavonoid Interactions with Human Transthyretin: Combined Structural and Thermodynamic Analysis. *J. Struct. Biol.* **2012**, *180*, 143–153. [[CrossRef](#)]
37. Cianci, M.; Folli, C.; Zonta, F.; Florio, P.; Berni, R.; Zanotti, G. Structural Evidence for Asymmetric Ligand Binding to Transthyretin. *Acta Cryst. D* **2015**, *71*, 1582–1592. [[CrossRef](#)]
38. Nilsson, L.; Larsson, A.; Begum, A.; Iakovleva, I.; Carlsson, M.; Brännström, K.; Sauer-Eriksson, A.E.; Olofsson, A. Modifications of the 7-Hydroxyl Group of the Transthyretin Ligand Luteolin Provide Mechanistic Insights into Its Binding Properties and High Plasma Specificity. *PLoS ONE* **2016**, *11*, e0153112. [[CrossRef](#)]
39. Genistein, a Natural Product from Soy, Is a Potent Inhibitor of Transthyretin Amyloidosis. Available online: <https://www.pnas.org/doi/10.1073/pnas.0501609102> (accessed on 7 March 2022).

40. Azeem, M.; Hanif, M.; Mahmood, K.; Ameer, N.; Chughtai, F.R.S.; Abid, U. An Insight into Anticancer, Antioxidant, Antimicrobial, Antidiabetic and Anti-Inflammatory Effects of Quercetin: A Review. *Polym. Bull.* **2022**. [[CrossRef](#)]
41. Tian, C.; Liu, X.; Chang, Y.; Wang, R.; Lv, T.; Cui, C.; Liu, M. Investigation of the Anti-Inflammatory and Antioxidant Activities of Luteolin, Kaempferol, Apigenin and Quercetin. *South Afr. J. Bot.* **2021**, *137*, 257–264. [[CrossRef](#)]
42. Ulusoy, H.G.; Sanlier, N. A Minireview of Quercetin: From Its Metabolism to Possible Mechanisms of Its Biological Activities. *Crit. Rev. Food Sci. Nutr.* **2020**, *60*, 3290–3303. [[CrossRef](#)]
43. Pawlowska, A.M.; Camangi, F.; Braca, A. Quali-Quantitative Analysis of Flavonoids of *Cornus mas* L. (Cornaceae) Fruits. *Food Chem.* **2010**, *119*, 1257–1261. [[CrossRef](#)]
44. Bruzual De Abreu, M.; Temraz, A.; Malafronte, N.; Gonzalez-Mujica, F.; Duque, S.; Braca, A. Phenolic Derivatives from *Ruprechtia polystachya* and their Inhibitory Activities on the Glucose-6-Phosphatase System. *Chem. Biodivers.* **2011**, *8*, 2126–2134. [[CrossRef](#)]
45. Iannuzzi, A.M.; Giacomelli, C.; Leo, M.D.; Russo, L.; Camangi, F.; Tommasi, N.D.; Braca, A.; Martini, C.; Trincavelli, M.L. *Cornus sanguinea* Fruits: A Source of Antioxidant and Antisenescence Compounds Acting on Aged Human Dermal and Gingival Fibroblasts. *Planta Med.* **2021**, *87*, 879–891. [[CrossRef](#)]
46. Razavi, S.M.; Zahri, S.; Zarrini, G.; Nazemiyeh, H.; Mohammadi, S. Biological Activity of Quercetin-3-O-Glucoside, a Known Plant Flavonoid. *Russ. J. Bioorg. Chem.* **2009**, *35*, 376–378. [[CrossRef](#)]
47. Zhang, X.; Thuong, P.T.; Jin, W.; Su, N.D.; Sok, D.E.; Bae, K.; Kang, S.S. Antioxidant Activity of Anthraquinones and Flavonoids from Flower of *Reynoutria sachalinensis*. *Arch. Pharm. Res.* **2005**, *28*, 22–27. [[CrossRef](#)]
48. Csepregi, K.; Neugart, S.; Schreiner, M.; Hideg, É. Comparative Evaluation of Total Antioxidant Capacities of Plant Polyphenols. *Molecules* **2016**, *21*, 208. [[CrossRef](#)]
49. Ciccone, L.; Nencetti, S.; Rossello, A.; Stura, E.A.; Orlandini, E. Synthesis and Structural Analysis of Halogen Substituted Fibril Formation Inhibitors of Human Transthyretin (TTR). *J. Enzym. Inhib. Med. Chem.* **2016**, *31*, 40–51. [[CrossRef](#)]
50. Oza, V.B.; Smith, C.; Raman, P.; Koepf, E.K.; Lashuel, H.A.; Petrassi, H.M.; Chiang, K.P.; Powers, E.T.; Sachtetinni, J.; Kelly, J.W. Synthesis, Structure, and Activity of Diclofenac Analogues as Transthyretin Amyloid Fibril Formation Inhibitors. *J. Med. Chem.* **2002**, *45*, 321–332. [[CrossRef](#)]
51. Ciccone, L.; Nencetti, S.; Tonali, N.; Fruchart-Gaillard, C.; Shepard, W.; Nuti, E.; Camodeca, C.; Rossello, A.; Orlandini, E. Monoaryl Derivatives as Transthyretin Fibril Formation Inhibitors: Design, Synthesis, Biological Evaluation and Structural Analysis. *Bioorganic Med. Chem.* **2020**, *28*, 115673. [[CrossRef](#)]
52. Yokoyama, T.; Kosaka, Y.; Mizuguchi, M. Inhibitory Activities of Propolis and Its Promising Component, Caffeic Acid Phenethyl Ester, against Amyloidogenesis of Human Transthyretin. *J. Med. Chem.* **2014**, *57*, 8928–8935. [[CrossRef](#)]
53. Ciccone, L.; Nencetti, S.; Rossello, A.; Tepshi, L.; Stura, E.A.; Orlandini, E. X-Ray Crystal Structure and Activity of Fluorenyl-Based Compounds as Transthyretin Fibrillogenesis Inhibitors. *J. Enzym. Inhib. Med. Chem.* **2016**, *31*, 824–833. [[CrossRef](#)]
54. Ciccone, L.; Vera, L.; Tepshi, L.; Rosalia, L.; Rossello, A.; Stura, E.A. Multicomponent Mixtures for Cryoprotection and Ligand Solubilization. *Biotechnol. Rep.* **2015**, *7*, 120–127. [[CrossRef](#)]
55. Ciccone, L.; Tepshi, L.; Nencetti, S.; Stura, E.A. Transthyretin Complexes with Curcumin and Bromo-Estradiol: Evaluation of Solubilizing Multicomponent Mixtures. *New Biotechnol.* **2015**, *32*, 54–64. [[CrossRef](#)]
56. Polsinelli, I.; Savko, M.; Rouanet-Mehouas, C.; Ciccone, L.; Nencetti, S.; Orlandini, E.; Stura, E.A.; Shepard, W. Comparison of Helical Scan and Standard Rotation Methods in Single-Crystal X-Ray Data Collection Strategies. *J. Synchrotron Radiat.* **2017**, *24*, 42–52. [[CrossRef](#)]
57. Polsinelli, I.; Nencetti, S.; Shepard, W.; Ciccone, L.; Orlandini, E.; Stura, E.A. A New Crystal Form of Human Transthyretin Obtained with a Curcumin Derived Ligand. *J. Struct. Biol.* **2016**, *194*, 8–17. [[CrossRef](#)]
58. Winn, M.D.; Ballard, C.C.; Cowtan, K.D.; Dodson, E.J.; Emsley, P.; Evans, P.R.; Keegan, R.M.; Krissinel, E.B.; Leslie, A.G.; McCoy, A. Overview of the CCP4 Suite and Current Developments. *Acta Crystallogr. Sect. D Biol. Crystallogr.* **2011**, *67*, 235–242. [[CrossRef](#)]
59. Adams, P.D.; Afonine, P.V.; Bunkóczi, G.; Chen, V.B.; Davis, I.W.; Echols, N.; Headd, J.J.; Hung, L.-W.; Kapral, G.J.; Grosse-Kunstleve, R.W. PHENIX: A Comprehensive Python-Based System for Macromolecular Structure Solution. *Acta Crystallogr. Sect. D Biol. Crystallogr.* **2010**, *66*, 213–221. [[CrossRef](#)]
60. Emsley, P.; Lohkamp, B.; Scott, W.G.; Cowtan, K. Features and Development of Coot. *Acta Crystallogr. Sect. D Biol. Crystallogr.* **2010**, *66*, 486–501. [[CrossRef](#)]
61. Moon, J.-K.; Shibamoto, T. Antioxidant Assays for Plant and Food Components. *J. Agric. Food Chem.* **2009**, *57*, 1655–1666. [[CrossRef](#)]
62. Ciccone, L.; Petrarolo, G.; Barsuglia, F.; Fruchart-Gaillard, C.; Cassar Lajeunesse, E.; Adewumi, A.T.; Soliman, M.E.S.; La Motta, C.; Orlandini, E.; Nencetti, S. Nature-Inspired O-Benzyl Oxime-Based Derivatives as New Dual-Acting Agents Targeting Aldose Reductase and Oxidative Stress. *Biomolecules* **2022**, *12*, 448. [[CrossRef](#)]
63. Montaña, M.; Cocco, E.; Guignard, C.; Marsh, G.; Hoffmann, L.; Bergman, Å.; Gutleb, A.C.; Murk, A.J. New Approaches to Assess the Transthyretin Binding Capacity of Bioactivated Thyroid Hormone Disruptors. *Toxicol. Sci.* **2012**, *130*, 94–105. [[CrossRef](#)]
64. Ciccone, L.; Tonali, N.; Shepard, W.; Nencetti, S.; Orlandini, E. Physiological Metals Can Induce Conformational Changes in Transthyretin Structure: Neuroprotection or Misfolding Induction? *Crystals* **2021**, *11*, 354. [[CrossRef](#)]
65. The GIMP Development Team *GIMP*; 2019.
66. Iacopini, P.; Baldi, M.; Storch, P.; Sebastiani, L. Catechin, Epicatechin, Quercetin, Rutin and Resveratrol in Red Grape: Content, in Vitro Antioxidant Activity and Interactions. *J. Food Compos. Anal.* **2008**, *21*, 589–598. [[CrossRef](#)]

- 
67. Dhouafli, Z.; Cuanalo-Contreras, K.; Hayouni, E.A.; Mays, C.E.; Soto, C.; Moreno-Gonzalez, I. Inhibition of Protein Misfolding and Aggregation by Natural Phenolic Compounds. *Cell. Mol. Life Sci.* **2018**, *75*, 3521–3538. [[CrossRef](#)]
  68. Amato, A.; Terzo, S.; Mulè, F. Natural Compounds as Beneficial Antioxidant Agents in Neurodegenerative Disorders: A Focus on Alzheimer's Disease. *Antioxidants* **2019**, *8*, 608. [[CrossRef](#)]